



# CHORUS

This is the accepted manuscript made available via CHORUS. The article has been published as:

## Emittance-Exchange-Based High Harmonic Generation Scheme for a Short-Wavelength Free Electron Laser

B. Jiang, J. G. Power, R. Lindberg, W. Liu, and W. Gai

Phys. Rev. Lett. **106**, 114801 — Published 16 March 2011

DOI: [10.1103/PhysRevLett.106.114801](https://doi.org/10.1103/PhysRevLett.106.114801)

# Emittance-Exchange-Based High Harmonic Generation Scheme for Short-Wavelength Free Electron Laser

*B. Jiang<sup>a,b</sup>, J.G. Power<sup>a</sup>, R. Lindberg<sup>a</sup>, W. Liu<sup>a</sup>, W. Gai<sup>a</sup>*

*a. Argonne National Laboratory, 9700 South Cass Avenue, Argonne, Illinois 60439, USA*

*b. Shanghai Institute of Applied Physics, CAS, Shanghai 201800, China*

Generation of short-wavelength radiation by a free electron laser using up-frequency conversion of an electron bunch density modulation is currently an area of active research. We propose a new scheme for producing the longitudinal electron bunch density modulation similar to the recently proposed echo-enabled harmonic generation but based on an emittance exchange beamline and a multislit mask. Beamline analysis and start-to-end simulation are presented.

PACS numbers: 29.27.-a, 41.60.Cr

The development of free-electron lasers (FELs) capable of generating short-wavelength radiation in the ultraviolet and soft x-ray regions is an area of active research. Two promising approaches are self-amplified spontaneous emission (SASE) FELs [1] and high-gain harmonic generation (HG) FELs [2]. However, both of them face some technical challenges. SASE radiation has rather poor temporal coherence and suffers from shot-to-shot fluctuations [3, 4] while HG radiation has limited frequency up-conversion capability. To address the later limitation, a cascaded HG scheme has been proposed to reach higher harmonics [5], but this approach is sensitive to timing jitter and requires high charge bunches [6].

Recently, an echo-enabled harmonic generation (EEHG) FEL scheme was proposed to generate radiation at unprecedented high harmonics of the seed laser. EEHG simulations presented in Ref. [7], and a demonstration experiment was done at SLAC observing 4<sup>th</sup> harmonic radiations [8]. The EEHG scheme (see Fig. 1(a)) uses two modulators to generate the longitudinal electron bunch density modulation. In “*modulator 1*,” the bunch first passes through a laser-seeded undulator, where it acquires an energy modulation, and second it passes through an over-bunched chicane to produce energy bands. “*Modulator 2*,” then converts the energy bands into a longitudinal density modulation at high harmonics of the seed laser.

It has recently become apparent to the accelerator community that the emittance exchange (EEX) beamline is useful beyond its original application of exchanging emittance between the longitudinal and transverse planes. Quite generally, it transforms features from the transverse plane into the longitudinal plane (and vice versa) and therefore has been used in a variety of applications [9-14]. In the original proposal [9], the EEX beamline is used to approximately exchange a smaller longitudinal emittance with a larger transverse one to improve the SASE performance. A modified scheme was found later [10] in which a full phase space exchange can be generated. More recently, an EEX beamline was used to generate longitudinal bunch trains and longitudinally ramped bunches [12, 13] from a transversely segmented bunch at the entrance to the EEX beamline. In this letter, we propose to use an EEX beamline as a part of a scheme to

generate short wavelength radiation from an FEL. The scheme we propose is comparable to EEHG-FEL (Fig. 1(a)) except in the method it uses to generate the energy bands. Despite the similarities, this scheme may deviate from what is meant by “echo”, so we call it the emittance exchange high-harmonic generation scheme (EEX-HHG).

The overall layout of the EEX-HHG scheme is shown in Fig. 1(b). An incident bunch is generated by the upstream accelerator (not shown), acquires energy bands when it passes through “*modulator 1*,” and obtains the longitudinal density modulation upon passing through “*modulator 2*.” Since *modulator 2* is identical to Ref. [7], we focus most of our discussion on *modulator 1* which consists of a multislit mask followed by an EEX beamline. We begin by presenting a single particle model of *modulator 1* to give the reader a clear picture of the underlying physics and justify this with a full numerical model at the end of the paper.

A multislit mask is used to segment the incident bunch into a series of beamlets separated in horizontal position at the entrance to the EEX beamline. The beamlets emerging from the mask are therefore distributed in a pattern of parallel lines and propagate into the EEX beamline. The dimensions of the metal slits can be quite challenging but nevertheless technically are achievable based on Ref. [15] and the heat load is negligible for typical repetition rates near 100 Hz.

The EEX beamline is used to transform particles initially separated in horizontal position into particles separated in energy at the exit. The beamline is composed of two dispersive sections (doglegs) with a RF deflecting cavity in between. Considering only the horizontal and longitudinal coordinates  $(x, x', z, \delta)$ , the transport matrix of the EEX beamline in the thick lens approximation can be found to be [11, 14]:

$$\begin{bmatrix} x_2 \\ x_2' \\ z_2 \\ \delta_2 \end{bmatrix} = \begin{bmatrix} 0 & L_c/4 & (\frac{L_c}{4}+L)k & -\frac{1}{k}+(\frac{L_c}{4}+L)k\xi \\ 0 & 0 & k & k\xi \\ k\xi & -\frac{1}{k}+(\frac{L_c}{4}+L)k\xi & \frac{L_c k^2 \xi}{4} & \frac{L_c k^2 \xi^2}{4} \\ k & (\frac{L_c}{4}+L)k & \frac{L_c k^2}{4} & \frac{L_c k^2 \xi}{4} \end{bmatrix} \begin{bmatrix} x_1 \\ x_1' \\ z_1 \\ \delta_1 \end{bmatrix}, \quad (1)$$

where the emittance exchange condition was used namely,  $1+\eta k=0$ .  $L, \eta, \xi$  are the length, dispersion, and momentum compaction of the dogleg respectively,  $L_c$  is the length of the cavity and  $k=(eV_0)/(aE_0)$  is the cavity strength parameter.  $V_0$  is the peak longitudinal RF voltage,  $a=\lambda/\pi$ ,  $\lambda$  is the wavelength of the  $TM_{110}$ -like mode and  $E_0$  is the mean bunch energy.

The longitudinal distribution at the exit of EEX beamline depends on both the initial horizontal distribution and the EEX beamline according to Eq. (1) as:

$$z_2 = k\xi x_1 + [-\frac{1}{k}+(\frac{L_c}{4}+L)\xi]kx_1' + \frac{L_c k^2 \xi}{4}(z_1 + \xi\delta_1), \quad (2)$$

$$\delta_2 = kx_1 + (\frac{L_c}{4}+L)kx_1' + \frac{L_c k^2}{4}(z_1 + \xi\delta_1), \quad (3)$$

where the subscripts 1, 2 refer to the location before and after EEX beamline respectively. For the scheme considered in this paper, our goal is to tune the incoming bunch phase space so that final energy and position  $(\delta_2, z_2)$  depends primarily on the initial horizontal position  $(x_1)$ . The last term on the r.h.s. of Eq. (2, 3) can be forced to zero by tuning the initial energy chirp to,

$$\delta_1 / z_1 = -1 / \xi, \quad (4)$$

where the upstream accelerator was used to place the chirp on the bunch. Next, the middle term in Eq. (2, 3) was made small in the following way. Given the EEX beamline parameters from Table I ( $k = 2.9 / m$ ,  $D = L_c / 4 + L \approx 1m$ , and  $\xi \approx -0.13m$ ), then we only need to satisfy

$$Dx'_1 / x_1 \ll 1. \text{ Using the Twiss parameter formalism, we have } Dx'_1 / x_1 = D\sqrt{\gamma / \beta} = D\sqrt{1 + \alpha^2} / \beta \text{ and we can express our condition as one that the initial transverse correlation must satisfy,}$$

$$D\sqrt{1 + \alpha^2} / \beta \ll 1. \quad (5)$$

This can easily be satisfied if  $\beta$  is large compared to  $D \cdot \alpha$ . For our design we chose (see Table II),  $\beta = 152m$ ,  $\alpha = 4$  so that  $Dx'_1 / x_1 = 0.03$ . Incidentally, the large  $\beta$  function is not only useful for creating well separated energy bands but also places less of a burden on fabrication of the multislit mask since the slits can be farther apart.

Based on the above analysis we see that *modulator 1* produces an energy modulated bunch by converting the horizontal position of the beamlets created by the mask ( $x_1$ ) into an energy position created by the EEX beamline ( $\delta_2$ ). Moreover, if the injected bunch has the energy chirp of Eq. (4) and the transverse phase space correlation of Eq. (5) then, using Eq. (2, 3), the output bunch can be shown to have acquired a linear energy chirp

$$\delta_2 / z_2 \approx 1 / \xi, \quad (6)$$

which is useful for compressing the bunch length and hence increasing the bunch current for the FEL application.

We now briefly describe how *modulator 2* converts the energy modulated bunch of *modulator 1* into longitudinal density modulations containing high-harmonics. A Fourier analysis of the longitudinal distribution of the bunch at the exit of *modulator 1* shows that it is modulated by  $\cos(2N\pi p)$ . Here  $p$  is the normalized energy spread  $p = (E - E_0) / \sigma_E$ ,  $\sigma_E$  is the energy spread of the bunch after *modulator 1*, and  $N$  is the number of energy bands per  $\sigma_E$ . Approximating the energy distribution to be a smoothly varying sinusoidal we have,

$$f_0(p) = \frac{1}{\sqrt{2\pi}} e^{-p^2/2} \cos(2N\pi p). \quad (7)$$

Following the method used in Ref. [7], the energy and position coordinates ( $z, p$ ) at the entrance to *modulator 2* are converted by the laser-seeded undulator and the chicane to the coordinates at the output of *modulator 2*:

$$z' = z + \frac{Bp}{q}, \quad (8)$$

$$p' = p + A\sin(qz), \quad (9)$$

where  $A = \Delta E / \sigma_E$ ,  $q$  is laser wave-number, and  $\Delta E$  is the bunch energy modulation produced by the laser,  $B = R_{56}q\sigma_E / E_0$  where  $R_{56}$  is dispersive strength of the chicane. The final longitudinal phase space distribution function can be found by combing Eq. (7-9),

$$f_1(p, z) = \frac{1}{\sqrt{2\pi}} e^{-\frac{[p - A\sin(qz - Bp)]^2}{2}} \cos(2N\pi[p - A\sin(qz - Bp)]). \quad (10)$$

And the longitudinal position distribution function is obtained by integrating  $f_1(p, z)$  over  $p$ ,

$$\rho(z) = \int_{-\infty}^{\infty} f_1(p) dp = \sum_{j=1}^{\infty} b_j \cos(jqz + \phi_j) + C. \quad (11)$$

where  $C$  represents the DC offset of the integral, and  $b_j$  is the amplitude of the  $j^{\text{th}}$  harmonic of the longitudinal distribution:

$$b_j \approx 2e^{-\frac{(Bj-2N\pi)^2}{2}} (1 + e^{-4N\pi Bj}) \left| J_j(2AN\pi) \right|. \quad (12)$$

The maximum value of this amplitude is approximately 2 and occurs when,  
 $j = \text{round}(2N\pi / B)$ , (13)

where the quantity  $\text{round}(n)$  denotes the integer nearest to  $n$ . Eq. (13) shows that one can control the location of the radiation spectrum peak by adjusting  $N$  and  $B$ , but we note that these values are constrained by practical considerations such as  $N$  must be large enough in order to fabricate the mask, etc. For comparison purposes, the amplitude of the peak harmonic in the EEHG scheme ( $c_k$  in Eq. (8) of Ref. [7]) depends on the laser strength  $A1$  which must be increased to create well separated energy bands.

As a practical example we carried out a study using the initial bunch parameters from the Fermi@elettra injector [16]. In *modulator 1*, the beam dynamics simulation in the EEX beamline were performed with PARMELA (including space charge effects) [17] and Matlab routines were written to handle the particles I/O at the mask and to apply the deflecting cavity thick lens matrix.

The bunch parameters from the Fermi@elettra injector are listed in Table II. The charge is reduced by the slits from 0.8 nC to 0.2 nC at location  $z1$  in Fig. 1(b) and as is the bunch current. The initial energy chirp was made to match the EEX energy chirp requirement (Eq. (4)). The initial **Twiss** parameters were chosen to satisfy two conditions: (i) the initial transverse correlation must satisfy Eq. (5); and (ii) as explained in [18], the **Twiss** parameters must be chosen to avoid emittance dilution in the EEX beamline (see Fig. 2(a)).

The EEX beamline parameters are listed in Table I. The energy bands at the exit of the *modulator 1* ( $z2$  in Fig 1(b)) are shown in Fig. 2(b) where the total *r.m.s.* energy spread is 0.23 MeV and the normalized transverse emittance is 5 mm·mrad. Recall that the bunch emerging from *modulator 1* is relatively easy to compress since it is already linearly chirped according to Eq. (6). Therefore, before entering *modulator 2*, we used a simple linear transformation to model the compression of the bunch by a chicane to 200fs and acceleration to 1.2 GeV (not shown). The phase space corresponding to this point ( $z3$  in Fig 1(b)) is shown in Fig. 2(c). Note that since the scale of the total bunch length is much longer than that of the laser wavelength only a small fraction of the bunch is sampled for the final phase-space plot after *modulator 2* as indicated by the thin rectangular box in Fig. 2(c). The longitudinal phase space after *modulator 2* ( $z4$  in Fig 1(b)) of this sampled region is shown in Fig. 2(d). Finally, projecting the phase space along the  $z$  axis reveals tens of spikes within one laser wavelength indicating the generation of very high harmonics.

To insure the robustness of EEX-HHG scheme we examined whether coherent synchrotron radiation (CSR) could smear out the bands and degrade the production of high harmonics using CSRtrack [19]. Note that CSR was only tracked in the “doglegs” of the EEX section to compare it to the EEHG scheme [7]. Fig. 3(a) shows the longitudinal phase space (with CSR) at the exit of the EEX. The induced energy spread ( $\sigma_{dE}$ ) from CSR is 30 keV. Comparing the CSR result of Fig. 3(a) to that of Fig. 2(b) we see that the energy bands remain mostly intact. We repeated the

CSR calculation in Fig. 3(b) for a smaller dogleg bending angle (smaller  $\eta$ ) which shows even less smearing of the bands. The downside of a small bend angle, according to emittance exchange condition ( $1+k\eta=0$ ), is that it requires higher  $k$  which places an additional burden on the deflecting cavity. In a real beamline design, a trade-off study would be made between CSR effects and the high-voltage capability of the deflecting cavity.

The final result was to send the density modulated bunch into the FEL using GINGER [20] for the simulation. The radiator beamline consists of several FODO sections and each FODO section has two 2.01 m long, 3 cm period undulators and two quadrupole-drift lines. Using a 400-nm seed laser, radiation power at the 24<sup>th</sup> harmonic (16.67nm wavelength) is plotted in Fig. 4 which shows that the power saturated at an undulator length of 16.5 m and 1 GW of peak power.

In summary, when the EEX-based energy-band generation scheme is combined with *modulator 2*, high harmonics of the seed laser can generate ultraviolet radiation. It is also possible (albeit more challenging) to obtain soft X-ray radiation using this scheme with a shorter-wavelength seed laser and a correspondingly smaller slit mask. A secondary benefit of the EEX based scheme is that it will generate a small transverse emittance provided the initial longitudinal emittance of the injected bunch is small. We have shown that CSR does not wash out the energy bands. Particle loss at the mask causes a reduction in current, but due to the linear energy chirp the bunch length can be compressed to restore the high peak bunch current needed by the FEL lasing condition.

The authors thank K.J. Kim for many useful discussions.

- 
- [1] R. Bonifacio, C. Pellegrini, and L.M. Narducci, Opt. Commun., **50**, 6 (1985).
  - [2] L.H. Yu, Phys. Rev. A **44**, 5178 (1991).
  - [3] K.-J. Kim, Nucl. Instrum. Methods Phys. Res., Sect. A **250**, 396 (1986).
  - [4] J.M. Wang and L.H. Yu, Nucl. Instrum. Methods Phys. Res., Sect A **250**, 484 (1986).
  - [5] Juhao Wu and L.H. Yu, Nucl. Instrum. Methods Phys. Res., Sect A **475**, 104 (2001).
  - [6] L.H. Yu, BNL-71229-2003-IR (2003).
  - [7] G. Stupakov, Phys. Rev. Lett., **102**, 074801 (2009).
  - [8] D. Xiang et al., Phys. Rev. Lett., **105**, 114801 (2010)
  - [9] M. Cornacchia and P. Emma, Phys. Rev. ST Accel. Beams **5**, 084001 (2002).
  - [10] K.-J. Kim and A. Sessler, AIP Conf. Proc. **821**, 115 (2006).
  - [11] P. Emma et al., Phys. Rev. ST Accel. Beams **9**, 100702 (2006).

- [12] P. Piot, Y.-E. Sun, and M. Rihaoui, Advanced Accelerator Concepts 13<sup>th</sup> workshop, 677 (2009).
- [13] Y.-E. Sun et al., Phys. Rev. Lett., **105**, 234801 (2010).
- [14] Y.-E. Sun et al., Proceedings of PAC07, New Mexico, USA, 3441-3443 (2007).
- [15] N. Delerue et al., Proceedings of PAC09, Vancouver, Canada, TH5RFP065 (2009).
- [16] C.J. Bocchetta et al., ELETTRA Report No. ST/F-TN-07/12 (2007).
- [17] J.H. Billen and L.M. Young, PARMELA Reference Manual, LA-UR-96-1835 (2000).
- [18] M. Rihaoui et al, AIP Conf. Proc. **1086**, 279 (2009).
- [19] M. Dohlus, A. Kabel, and T. Limberg, Nucl. Instrum. Methods Phys. Res., Sect A **445**, 338 (2000).
- [20] W.M. Fawley, Lawrence Berkeley National Laboratory, LBNL-49625-Rev.1 (2004).

TABLE I. Modulator 1 parameters of the EEX-HHG design.

Total number of slits	25
Slits width / space	50 / 200 $\mu\text{m}$
Dogleg bend length	0.2 m
Drift space between bends	0.6 m
Bending angle	22 degrees
Deflecting cavity length	0.2 m
Deflecting cavity strength k	2.9 /m
Dispersion $\eta$	-0.35 m
Momentum compaction $\xi$	-0.13m

TABLE II. Initial bunch parameters used in the simulation (data borrowed from the Fermi@elettra injector, with the exception of optimized bunch length and **Twiss** parameters).

Bunch energy	95 MeV
Bunch charge	0.8 nC
Normalized emittance (x / z)	1.5 / 3.7 $\mu\text{m}$
Bunch size, x (RMS)	1.1 mm
Energy spread (uncorrelated / correlated)	2 KeV / $\sim$ 150 KeV
Bunch length	700 fs
$\beta$ / $\alpha$ function	152 m / 4.0

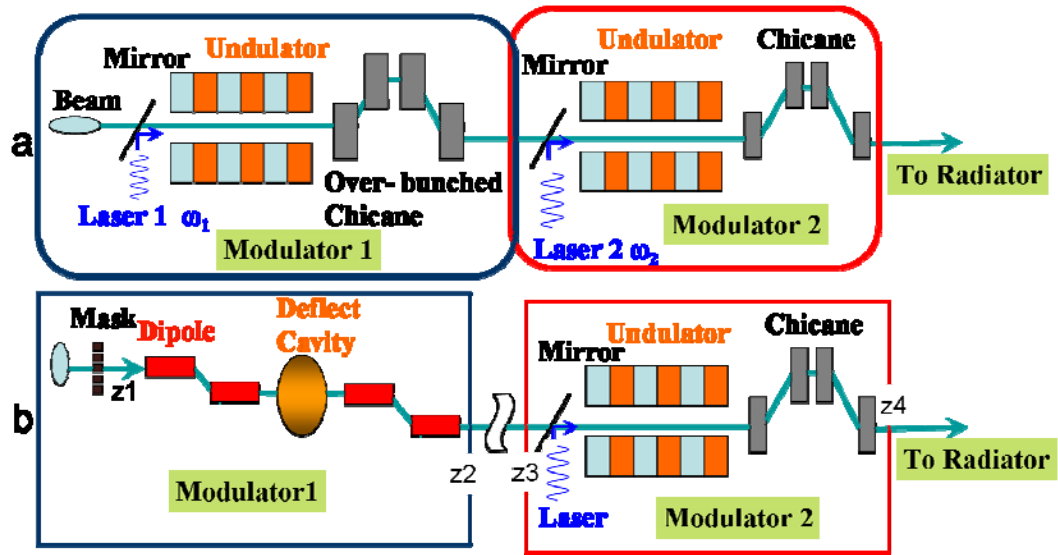


FIG. 1. Illustration of the EEHG-FEL scheme (a) and the EEX-HHG FEL scheme (b).

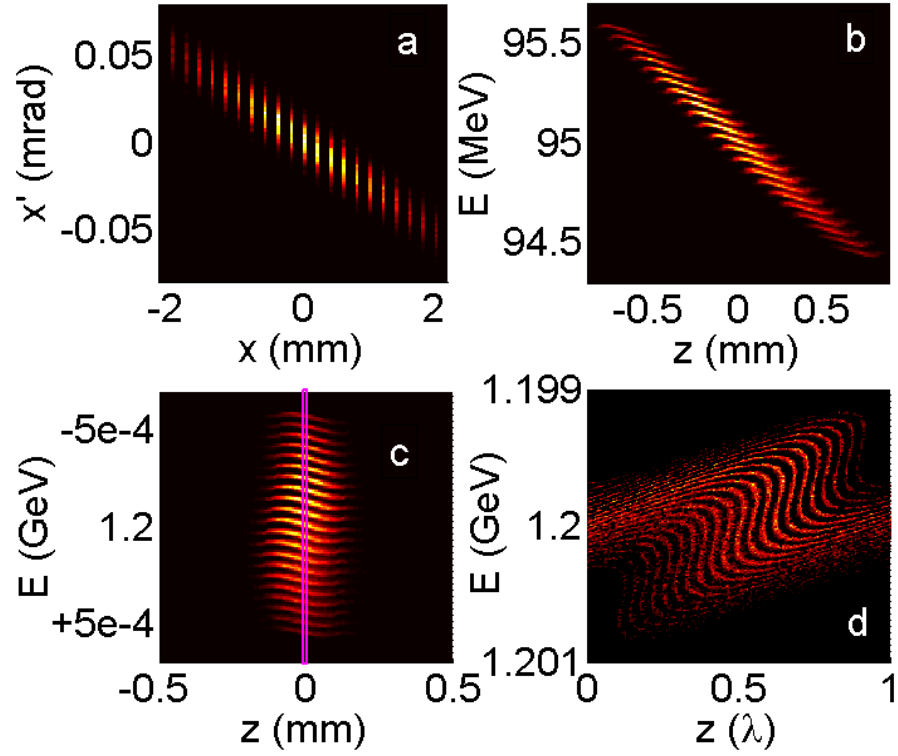


FIG. 2. Simulation results at different locations of EEX-HHG beamline corresponding to the locations in Fig 1: (a) bunch transverse phase space after mask at  $z_1$  in Fig. 1; (b) energy bands created by EEX at  $z_2$  in Fig. 1; (c) bunch after further acceleration and length compression at  $z_3$  in Fig. 1; (d) density modulation by the modulator 2 at  $z_4$  in Fig. 1.

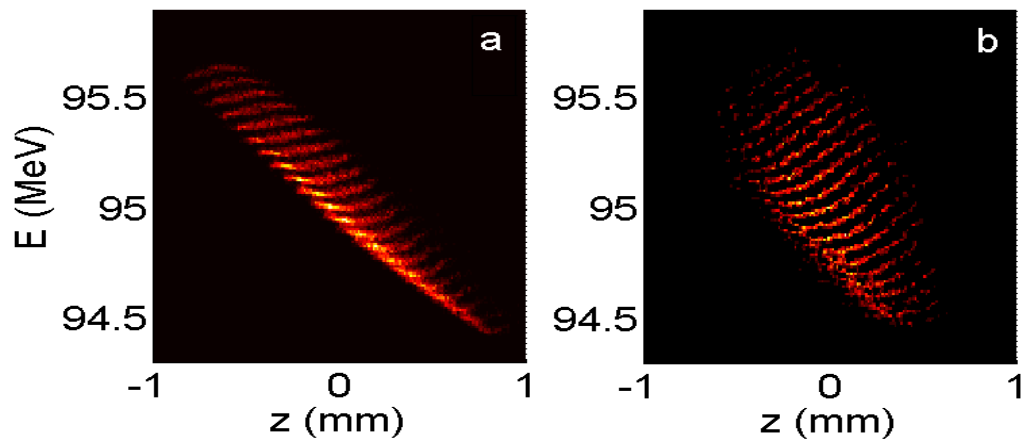


FIG. 3. CSR effect in EEX with different bending angles: (a) 22 degrees; (b) 12 degrees.

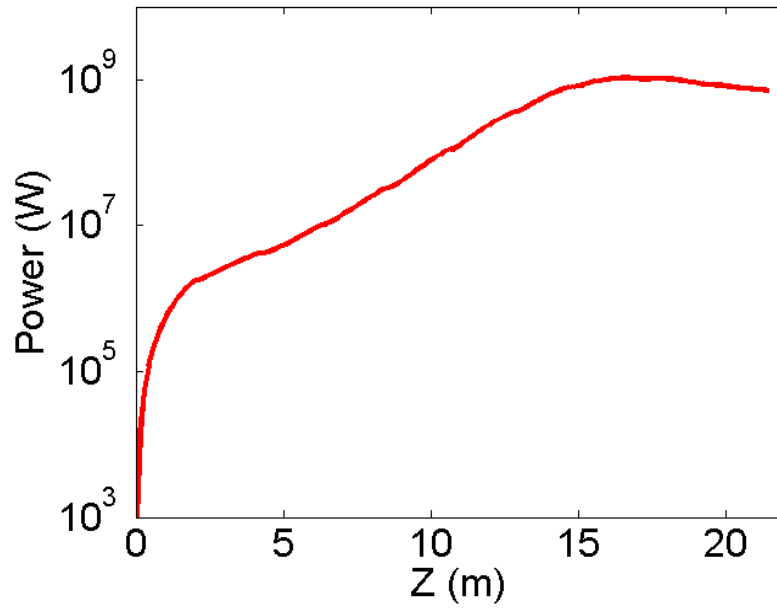


FIG. 4. FEL power evolution through the undulator.